Vision Research 160 (2019) 72–81

Contents lists available at ScienceDirect

Vision Research

journal homepage: www.elsevier.com/locate/visres

Melanopsin driven enhancement of cone-mediated visual processing

Andrew J. Zele[a,b,*], Prakash Adhikari[a,b], Dingcai Cao[d], Beatrix Feigl[a,c,e]

[a] Institute of Health and Biomedical Innovation, Queensland University of Technology (QUT), 60 Musk Avenue, Brisbane QLD 4059, Australia
[b] School of Optometry and Vision Science, Queensland University of Technology (QUT), Australia
[c] School of Biomedical Sciences, Queensland University of Technology (QUT), Australia
[d] Department of Ophthalmology and Visual Sciences, University of Illinois at Chicago, 1855 West Taylor Street, Chicago IL 60612, USA
[e] Queensland Eye Institute, Brisbane, Australia

ARTICLE INFO

Keywords:
Melanopsin
Chromatic discrimination
Colour vision
Cone photoreceptors
Intrinsically photosensitive retinal ganglion cells

ABSTRACT

The precise control of visual sensitivity to variations in external lighting is critical for optimising human visual function in a changing environment. In photopic illumination, the cone photoreceptors and their post-receptoral pathways have a primary role in regulating these adjustments; it is not fully understood how a small population of melanopsin-expressing, intrinsically photosensitive retinal ganglion cells (ipRGCs) can interact with the three cone photoreceptor classes to modulate human visual function. Here we investigated interactions between these inner and outer retinal photoreceptor classes in participants with trichromatic colour vision under conditions that independently controlled the excitations of ipRGCs, cones and rods in the retina. In the peripheral retina, we show that interaction between melanopsin- and cone-directed signals affect conscious, image-forming vision. The interaction patterns are inconsistent with any potential effects arising from artefacts due to open-field and penumbral-cone contrasts, or rod intrusion. For cone signals mediated via each of the three primary visual pathways, melanopsin activation enhances contrast sensitivity. The contrast response functions indicate this enhancement is a more generalised facilitation effect that onsets at ~9% melanopsin contrast. The implication for human vision is that the contrast sensitivity of cone-mediated visual processes can be modulated by the level of melanopsin excitation in the stimulus light.

1. Introduction

The detection of variations in image contrast in daylight illumination has long been considered the domain of visual pathways originating with cone photoreceptors. The discovery of melanopsin-expressing intrinsically photosensitive retinal ganglion cell (ipRGCs) projections to multiple brain regions for image- and non-image forming vision has brought this view into question. Melanopsin cells (ipRGCs) project to the dorsal lateral geniculate nucleus (dLGN) in non-human primates (Dacey et al., 2005; Hannibal et al., 2014), a relay centre to cortical centres for image-forming vision where melanopsin-directed light stimulation may produce haemodynamic changes in the activity of human visual area 1 (V1) (Spitschan et al., 2017). In peripheral retina, a tetrachromatic theory maybe required to account for visual sensitivity (Horiguchi, Winawer, Dougherty, & Wandell, 2013), with melanopsin photoreception potentially giving rise to a dimension of vision independent from rods and cones (Zele, Feigl, Adhikari, Maynard & Cao, 2018) that interacts with these canonical photoreceptors to influence non-visual, pupil control (Adhikari, Feigl, & Zele, 2016; Barrionuevo et al., 2014; Cao, Nicandro, & Barrionuevo, 2015; Gamlin et al., 2007; Gooley et al., 2012; Spitschan, Jain, Brainard, & Aguirre, 2014; Zele, Feigl, Smith, & Markwell, 2011). Any contributions of melanopsin to human vision must be separated from the exquisite contrast sensitivity of cone-mediated visual processes (Cao et al., 2015; Horiguchi et al., 2013; Spitschan et al., 2017; Zele, Feigl et al., 2018). When this separation is achieved, melanopsin photoreception in people with trichromatic colour vision is $> 10\times$ less sensitive than red-green chromatic vision, with temporal resolution to ~5 Hz and an S-off L + M-on colour response property (Zele, Feigl et al., 2018) that matches the receptive field identified in macaque retina (Dacey et al., 2005). With lower sensitivity than the principal cone pathways, there arises the question of how might melanopsin interact with cone signals to influence photopic visual function.

Rudimentary spatial vision is possible in melanopsin only, rod-cone knockout mice (Ecker et al., 2010); in the wild-type, melanopsin activation enhances visual encoding of spatial patterns (Allen, Storchi,

* Corresponding author at: Visual Science Laboratory, Institute of Health and Biomedical Innovation, QUT. 60 Musk Avenue, Kelvin Grove, Queensland 4059, Australia.
E-mail address: andrew.zele@qut.edu.au (A.J. Zele).

https://doi.org/10.1016/j.visres.2019.04.009
Received 13 December 2018; Received in revised form 16 April 2019; Accepted 21 April 2019
Available online 21 May 2019
0042-6989/

Martial, Bedford, & Lucas, 2017) whereas melanopsin null mice have reduced behavioural contrast sensitivity (Schmidt et al., 2014). The significance of such interactions between melanopsin and cones for human vision is yet to be established. In humans, melanopsin has a role in brightness perception through its combined contribution with cone signalling (Brown et al., 2012; Zele, Adhikari, Feigl & Cao, 2018). We therefore examine how melanopsin activation affects a principal cone-mediated visual function, namely the capacity for contrast discrimination of lights mediated via the three cone pathways; one for luminance information through an additive combination of the +L + M cones, and two for chromatic information for red-green (+L − M cone) and blue-yellow (S − (L + M cone)) vision. When one of these three pathways is selectively chromatically adapted, the sensitivity of the other two pathways remains largely unaffected (Krauskopf, Williams, & Heeley, 1982), indicating independence of these processes, at least in the early visual pathways. Here we establish that cone-mediated contrast discrimination is dependent on the level of melanopsin excitation in the stimulus light.

2. Materials and methods

2.1. Participants and ethics statement

Experimental protocols were approved by the Queensland University of Technology (QUT) Human Research Ethics Committee (approval no: 1700000510) and completed in accordance with their stipulations. Test protocols were conducted in observance of the tenets of the Declaration of Helsinki; all participants provided informed consent after explanation of the nature and possible consequences of the experiments. Five people with trichromatic colour vision (2 females, 3 males, 23–41 years) and one deuteranomalous trichromat (male, 34 years) participated in accordance with the human research ethics approval. Observer O1 was an Author. All observers underwent a comprehensive ophthalmic examination, including fundus examination, ocular coherence tomography, colour vision (Rayleigh colour match and D-15), contrast sensitivity (Pelli-Robson), visual acuity, and intra-ocular pressure to exclude any retinal or optic nerve disease.

2.2. Apparatus and calibrations

All test stimuli were generated with a calibrated five-primary Maxwellian-view photostimulator having 12-bit resolution and a ~488 Hz upper frequency limit (Cao et al., 2015). The photostimulator includes five narrowband primary lights comprising light emitting diodes (LED) and interference filters with peak wavelengths (full widths at half maximum) at 456 nm (10 nm), 488 nm (11 nm), 540 nm (10 nm), 594 nm (14 nm), and 633 nm (15 nm) that were combined using fibre optic cables and homogeniser and focussed by an achromatic doublet field lens in the plane of a 2 mm artificial pupil in Maxwellian view. The primary lights were controlled by an Arduino based stimulation system, LED driver (TLC5940), microcontroller (Arduino Uno SMDR3, Model A000073) and calibrated neutral density filters (Ealing, Natick, MA, USA) using custom engineered software (Xcode 3.2.3, 64-bit, Apple, Inc., Cupertino, CA, USA). Spectral outputs of five primary lights were measured with a spectroradiometer (StellarNet, Tampa, FL, USA); luminance outputs measured with an ILT1700 Research Radiometer (International Light Technologies, Inc., Peabody, MA, USA) as a function of the duty cycle of the LED driver were used to compute the linearisation coefficients (Cao et al., 2015).

The excitation of melanopsin, rhodopsin and the three cone opsins were independently controlled according to the principle of silent substitution (Cao et al., 2015; Estévez & Spekreijse, 1982). The L- M- and S-cone, rod (R) and ipRGC (i) excitations were calculated based on CIE 1964 10° standard observer cone fundamentals of (Smith & Pokorny, 1975), the CIE 1951 scotopic luminosity function, and melanopsin spectral sensitivity function (Adhikari, Zele, & Feigl, 2015; Enezi et al., 2011), respectively. For a 1 photopic Troland (Td) light metamteric to an equal energy spectrum, the photoreceptor excitation relative to photopic luminance with a 2:1 L:M cone ratio is $l = L/(L + M) = 0.6667$, $m = M/(L + M) = 0.3333$, $s = S/(L + M) = 1$, $r = R/(L + M) = 1$, $i = I/(L + M) = 1$ (where i is the intrinsic melanopsin response). This specification of stimulus chromaticities in a relative cone-Troland space (Boynton & Kambe, 1980) plots l versus s, the two cardinal axes in a MacLeod and Boynton equiluminant cone chromaticity space that allows comparison of detection and discrimination data in terms of the quantal excitation of the photoreceptors and which correspond to the PC and KC pathways (Lee, Pokorny, Smith, Martin, & Valberg, 1990). To obtain the maximum instrument gamut for the photoreceptor-isolating conditions, the 2000 photopic Td adapting stimulus field chromaticity was an orange appearing field ($l = 0.752$, $s = 0.105$, $r = 0.319$ and $i = 0.235$).

To nullify individual differences in pre-receptoral filtering and photoreceptor spectral sensitivities between the observer and the CIE 1964 10° standard observer, participants performed heterochromatic flicker photometry (HFP) settings between a reference primary (cyan; 15 Hz square wave counterphase flicker, 100 Td mean illuminance) and each of the test primaries (blue, green, amber and red). We performed HFP settings at 100 Td because they more precisely estimate luminous efficiency (Vλ) than those measured at higher illuminations (Pokorny, Jin, & Smith, 1993). The 15 Hz flicker is likely mediated by the inferred luminance pathway (Guth & Lodge, 1973; Smith & Pokorny, 1975) because the modulation frequency is beyond the temporal resolution of both the chromatic mechanisms (Brindley, Du Croz, & Rushton, 1966; Swanson, Ueno, Smith, & Pokorny, 1987) and of melanopsin photoreception (Zele, Feigl et al., 2018) at the 100 Td retinal illuminance. For each wavelength combination, the observer was required to minimise the appearance of flicker by controlling the radiance of the test primary using a method of adjustment. The final setting for each test-reference wavelength combination was defined as the average of 15 repeats; the theoretical 10° standard observer data was then scaled by the observer's average HFP settings. For a workable system of photometry, the Vλ function should provide a reasonable assessment of the spectral sensitivity of human vision across a wider range of conditions than in which it was initially estimated (CIE, 1994). The generality of colour matching data for conditions other than in which they were measured, is encapsulated in the trichromatic generalisation and Grassman's laws; the estimated luminance efficiency function is expected to be applicable at higher illuminations given that Rayleigh colour matches remain stable up to ~8000 Td (Burns, Elsner, Lobes, & Doft, 1987). Given the importance of the precision of the estimates of an individual spectral sensitivity on our measurements, and their dependence on the viewing conditions (Burns & Elsner, 1993; Pokorny et al., 1993; Wright, 1936), including the background chromaticity (Sharpe, Stockman, Jagla, & Jägle, 2010), further studies should investigate the generality of the HFP procedure to provide a silent substitution for luminance when using different adaptation conditions.

2.3. Experimental design: psychophysical paradigms

The stimulus was a 30° diameter circular field with the central 10.5° blocked to eliminate the effect of macular pigment. A small hole (< 1 min arc) within the centre of the macular blocker was used to guide fixation. Observers were adapted to the dark-room illumination (< 0.0003 lx) for 15 min prior to all experimental sessions which followed with a 2-minute adaptation to the 2000 Td orange field. We investigated five photoreceptor combinations: [1] melanopsin-directed stimuli with no change in the excitation of the rods and three cone types, [2] L- and M-cones modulated in-phase to produce a cone luminance increment (+L + M) or decrement (−L − M) with no change in the excitation of S-cones, rods or melanopsin, [3] S-cone increments and decrements (+S, −S) with no change in the excitation of melanopsin, rods, L- and M-cones, [4] a counterphase equiluminant L- and

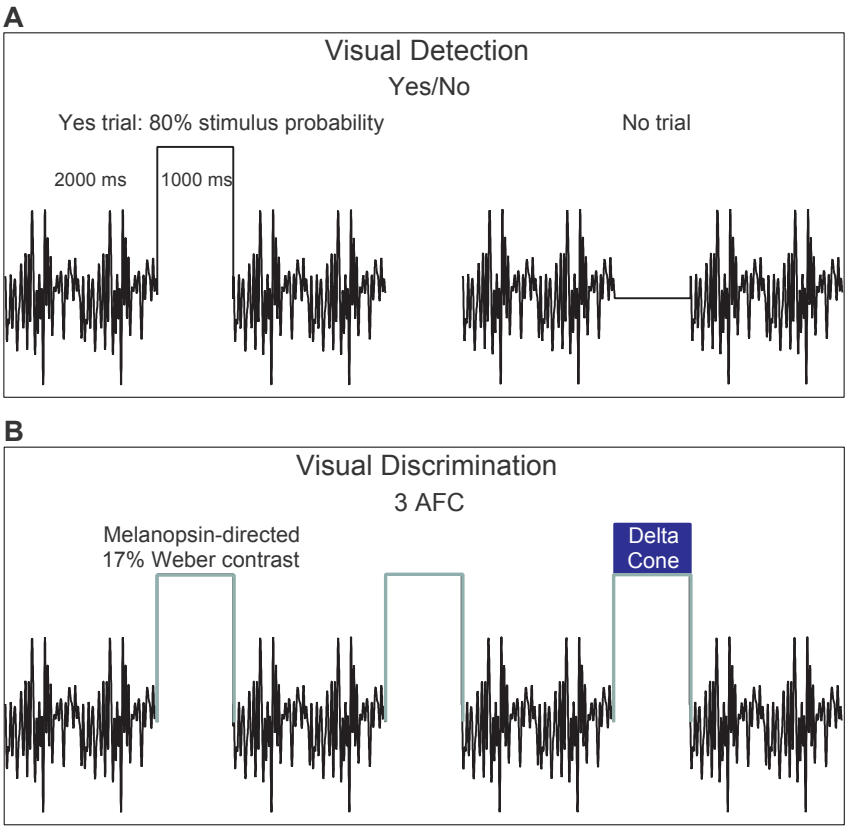

Fig. 1. Contrast detection and discrimination tasks. (A) Visual detection thresholds were measured separately for melanopsin, +L + M cone luminance, S-cones and red-green (+L − M) equiluminant chromatic modulations. A pilot experiment showed that cone detection thresholds were similar when measured with the yes/no and 3-alternative forced choice (3-AFC) procedures and so the detection data were collected using the more efficient yes/no paradigm. (B) To study melanopsin interaction with cones, contrast discrimination thresholds were measured along the three canonical visual directions using a 3-AFC procedure with and without a 17% Weber contrast increment in the melanopsin excitation. Rod excitation was constant in all conditions. The stimulus duration was 1000 ms with a 2000 ms inter-stimulus interval during which time the temporal white noise (TWN) randomly modulated the S-cone, M-cone, L-cone and Rod photoreceptor excitations (40% Michelson contrast) (Hathibelagal et al., 2016; Zele et al., 2017) without changing the melanopsin photoreceptor excitation (Zele, Feigl et al., 2018b). (For interpretation of the references to colour in this figure legend, the reader is referred to the web version of this article.)

M-cone modulation (+L − M, −L + M) with no change in L + M cone luminance or the excitation of S-cones, rods or melanopsin, and [5] the additive mixture of melanopsin with each of the photoreceptor combinations specified in [2] to [4].

Visual detection thresholds (1000 ms incremental stimulus; three-alternative forced choice procedure) were measured separately for melanopsin, L + M cone luminance, S-cones and red-green (+L − M) equiluminant chromatic modulations (Fig. 1) at 2000 photopic Td (~15.1 log quanta.cm^{-2}.s^{-1} corneal irradiance) using a double alternating, yes-no staircase psychophysical procedure with 80% stimulus probability (Zele, Smith, & Pokorny, 2006). Rod excitation was constant in all conditions. The inter-stimulus interval (ISI) was 2000 ms and included temporal white noise (TWN) that randomly modulated the S-cone, M-cone, L-cone and rod photoreceptor excitations (40% Michelson contrast) (Hathibelagal, Feigl, Cao, & Zele, 2018; Hathibelagal, Feigl, Kremers, & Zele, 2016; Zele et al., 2017) without changing the melanopsin photoreceptor excitation (Zele, Feigl et al., 2018); details of the temporal white noise are given in Section 2.5. To determine the melanopsin interactions with the canonical cone pathways for image forming vision (as per condition 5, above), cone discrimination thresholds were re-measured in the presence of a melanopsin incremental pedestal (17% Weber contrast). All stimulus conditions were randomised. These contrast discrimination data were modelled using a quadratic, line element energy model with three processes, two chromatically opponent and one additive. The effect of the non-melanopsin photoreceptor absorptions on contrast discrimination were quantified in additional experiments using spatially and temporally co-extensive increment pedestals, one that selectively simulated the penumbral cone contrast in the melanopsin-directed stimulus and a second that simulated the open-field cone contrast (see Section 2.4).

2.4. Computation of the open-field cone contrast and penumbral cone contrast in the theoretical melanopsin-directed stimulus

On completion of the physical light calibrations of the photostimulator, a theoretical melanopsin-directed stimulus (β = [S M L R I] = [0.105 0.248 0.752 0.319 0.275]; 17% melanopsin Weber contrast) was generated by appropriately scaling the maximum output of the five primary lights according to α = [b c g a r], where b, c, g, a, r are the scaled outputs of the spectral distributions of the B_λ = blue, C_λ = cyan, G_λ = green, A_λ = amber and R_λ = red primaries (Cao et al., 2015; Shapiro, Pokorny, & Smith, 1996; Zele, Feigl et al., 2018). Photoreceptor excitations β = [S M L R I] were calculated using linear algebra where β = αA and A is a matrix (Eq. (1)) with each row representing the photoreceptor excitations [S M L R I: S-cones, M-cones, L-cones, rods (R) and melanopsin (I); (Adhikari et al., 2015; Enezi et al., 2011; Smith & Pokorny, 1975)] at the maximum output of each primary [B C G A R],

$$A = \begin{bmatrix} S_B & M_B & L_B & R_B & I_B \\ S_C & M_C & L_C & R_C & I_C \\ S_G & M_G & L_G & R_G & I_G \\ S_A & M_A & L_A & R_A & R_A \\ S_R & M_R & L_R & R_R & I_R \end{bmatrix} \quad (1)$$

and the unique scaling coefficients of the primary lights for any theoretical photoreceptor excitation are defined in Eq. (2) as

$$\beta = \alpha A \quad (2)$$

To estimate the level of open-field cone intrusion, with the theoretical melanopsin-directed stimulus, the *s m l r i* photoreceptor excitations were calculated using the irradiances of the five primary lights measured with an EPP2000C-50 μm Slit UV–VIS Spectrometer (StellarNet, Tampa, FL, USA). The α in Eq. (2) was replaced with the measured spectral irradiance of the theoretical stimulus and the open-

field cone intrusion into the melanopsin pulse was defined as the differences between the theoretical and measured S M L R I photoreceptor excitations as given in Eq. (3), where

$$[smlri] = [bcgar] \times \begin{bmatrix} \frac{S_B}{L_B+M_B} & \frac{M_B}{L_B+M_B} & \frac{L_B}{L_B+M_B} & \frac{R_B}{L_B+M_B} & \frac{I_B}{L_B+M_B} \\ \frac{S_C}{L_C+M_C} & \frac{M_C}{L_C+M_C} & \frac{L_C}{L_C+M_C} & \frac{R_C}{L_C+M_C} & \frac{I_C}{L_C+M_C} \\ \frac{S_G}{L_G+M_G} & \frac{M_G}{L_G+M_G} & \frac{L_G}{L_G+M_G} & \frac{R_G}{L_G+M_G} & \frac{I_G}{L_G+M_G} \\ \frac{S_A}{L_A+M_A} & \frac{M_A}{L_A+M_A} & \frac{L_A}{L_A+M_A} & \frac{R_A}{L_A+M_A} & \frac{I_A}{L_A+M_A} \\ \frac{S_R}{L_R+M_R} & \frac{M_R}{L_R+M_R} & \frac{L_R}{L_R+M_R} & \frac{R_R}{L_R+M_R} & \frac{I_R}{L_R+M_R} \end{bmatrix} \quad (3)$$

Following Eq. (3), we determined that for a 17% melanopsin-directed increment on a 2000 Td adaptation field, the (physical) open-field L-, M- and S-cone contrasts were 0.0%, 0.1% and 1.3%, respectively, and the rod contrast was 0.3%. In the cone isolating conditions, the rod contrast was always $\leq$0.3%.

To estimate the effect of light absorption by the retinal vasculature on the photoreceptor isolation, the spectral irradiance of each primary received by penumbral cones was determined using calculations detailed elsewhere (Horiguchi et al., 2013; Spitschan, Aguirre, & Brainard, 2015; Zele, Feigl et al., 2018). Briefly, the open-field spectral irradiances or the calculated penumbral spectral irradiances were used in Eq. (1) to calculate the open-field or penumbral $s\ m\ l\ r\ i$ excitations in Eq. (3). The penumbral cone contrasts were defined as the differences between the open-field and penumbral $s\ m\ l\ r\ i$ excitations. For the 17% melanopsin-directed pulse on a 2000 Td adaptation field, the penumbral L-, M- and S-cone contrasts were 0.2%, 0.5% and 0.6%, respectively, and the rod contrast was 0.2%. In the cone isolating conditions, the rod contrast was always $\leq$0.3%.

2.5. Temporal white noise (TWN) to desensitise penumbral cones

Our theoretical calculations for specifying the photoreceptor-directed stimuli were based on open-field cones and so there arises a possibility that penumbral cones in the shadow of the retinal vasculature may intrude in the measurements using melanopsin-directed stimuli (Horiguchi et al., 2013; Spitschan et al., 2015; Zele, Feigl et al., 2018). Any effect of penumbral cones on the photoreceptor isolation was therefore eliminated by presenting, before and after the test stimuli, TWN that modulated the L-, M-, S-cone and rod excitations (without changing the melanopsin excitation) (Zele, Feigl et al., 2018). Details of temporal white noise and evidence of its effectiveness in desensitising penumbral cones are given elsewhere; this cone- and rod-directed TWN has no effect on melanopsin-directed visual contrast sensitivity (Zele, Feigl et al., 2018).

2.6. Confirmation of photoreceptor isolation

The accuracy of the observer calibration and photoreceptor isolation was confirmed via multiple control measurements using the same stimulus spatial configuration initially described in Section 2.3; Firstly, a rod incremental pulse (500 ms, 18% Weber contrast) with no change in the melanopsin or cone excitations at a 5 Troland (Td) adaptation level was highly conspicuous after dark adaptation, but invisible after photopigment bleach. Secondly, this rod incremental pedestal was perceptually equivalent to a decrease in L/[L + M], an increase in S/[L + M] and an increase in [L + M] as previously reported for rod-directed stimuli (Cao, Pokorny, Smith, & Zele, 2008). Thirdly, the rod incremental pulse was invisible when presented at the maximum achievable contrast (18%) at a 5000 photopic Td adaptation level. Finally, after 30 min of dark-adaptation, we evaluated the effect of potential stimulus artefacts in the melanopsin-, rod- and cone-directed stimuli by measuring frequency of seeing at four adaptation levels spanning the scotopic to mesopic transition (0.02 Td, 0.2 Td, 2 Td, and 20 Td). The stimuli were 1000 ms duration (18% contrast; 2000 ms ISI; no temporal white noise) melanopsin-directed, rod-directed or L + M cone-directed incremental pulses that were randomly interleaved (24 trials per stimulus) with blank, catch trials (18 trials; 20% probability). The hit rate (HR) was defined as the proportion of yes responses for each of the three stimulus types and the false alarm (guess) rate (GR) was defined as the proportion of yes responses to the catch trails; frequency of seeing was therefore defined as $[1 - \{(1 - HR)/(1 - GR)\}]$*100% (Pelli, 1985). Of note, the photoreceptor-directed stimuli used in this study also give rise to pupil light responses having different amplitude and timings, consistent with mediation via different visual processes (Barrionuevo & Cao, 2016; Zele, Adhikari, Cao, & Feigl, 2019).

Individual differences in luminous efficiency, including any effect from photoreceptor polymorphisms, were corrected for during the HFP observer calibration, as were lens density (Cao et al., 2015); the inclusion of data from an anomalous trichromat provides a direct test of this. To evaluate the effectiveness of the individual observer calibration in limiting the effect of polymorphisms on the peak of the spectral sensitivity, a deuteranomalous observer completed select conditions with and without the individual observer calibration. We hypothesised that when a deuteranomalous observer completes the experiments with the standard observer calibration, the silent substitution will be incomplete due to the presence of the shifted M-cone photopigment sensitivity towards the L-cone, which also displaces the luminous efficiency function V(λ) to longer wavelengths; it follows that a deuteranomalous trichromat using a standard observer calibration would return a lower melanopsin-directed visual threshold, due to cone-intrusion in the stimulus.

3. Results

With a constant melanopsin excitation at the adaptation level, detection thresholds for the three primary cone directions (Fig. 2, black symbols) show the anticipated ellipse orientation and higher sensitivity of the chromatically opponent (+L − M) process compared to the additive (L + M) luminance and S-cone directions (Boynton & Kambe, 1980; Cole, Hine, & McIlhagga, 1993; Horiguchi et al., 2013; Krauskopf et al., 1982; Zele et al., 2006). Detection thresholds for melanopsin-directed stimuli measured in temporal white noise (mean ± SEM; 14.1% ± 0.6 Weber contrast) are higher than those for the principal cone-directions; 2.0× S-directed thresholds, 2.4× luminance (L + M) thresholds and 67.1× chromatic (L − M) thresholds (Fig. 3A). The colour appearance of the melanopsin-directed stimulus was verbally reported by participants as having an orangish appearance (two trichromats) or a bluish-cyanish appearance (three trichromats and one deuteranomalous trichromat).

If cone processing is independent of the melanopsin excitation level, cone thresholds should be invariant to changes in the strength of the melanopsin signal. To test this hypothesis, chromatic discrimination was re-measured in the presence of a higher melanopsin excitation (17% contrast). We observe that melanopsin excitation enhances cone-mediated visual discrimination by reducing the ellipse area without changing the orientation (Fig. 2, orange symbols). Ellipse areas show an average decrease (n = 3 observers) of −57.8% ± 7.2 SEM for modulations along the L- and M-cone axes (Fig. 2, left column), −61.2% ± 5.8 for L- and S-cone modulations (middle column) and −60.6% ± 6.3 for M- and S-cone modulations (right column). This relative percentage enhancement is evident for the cone luminance directed (n = 5 observers: Δ + L + M threshold = 25.57% ± 5.06 SEM; Δ − L − M threshold = 35.21% ± 9.64), S-cone directed (Δ + S threshold = 31.61% ± 6.64; Δ − S threshold = 23.36% ± 5.61) and the red-green chromatic directed stimuli (Δ + L − M threshold = 35.21% ± 9.64; Δ − L + M threshold 17.54% ± 7.39) (Fig. 3B).

Cone thresholds were found to be dependent on the level of melanopsin excitation, and so we evaluated if the change in cone-mediated

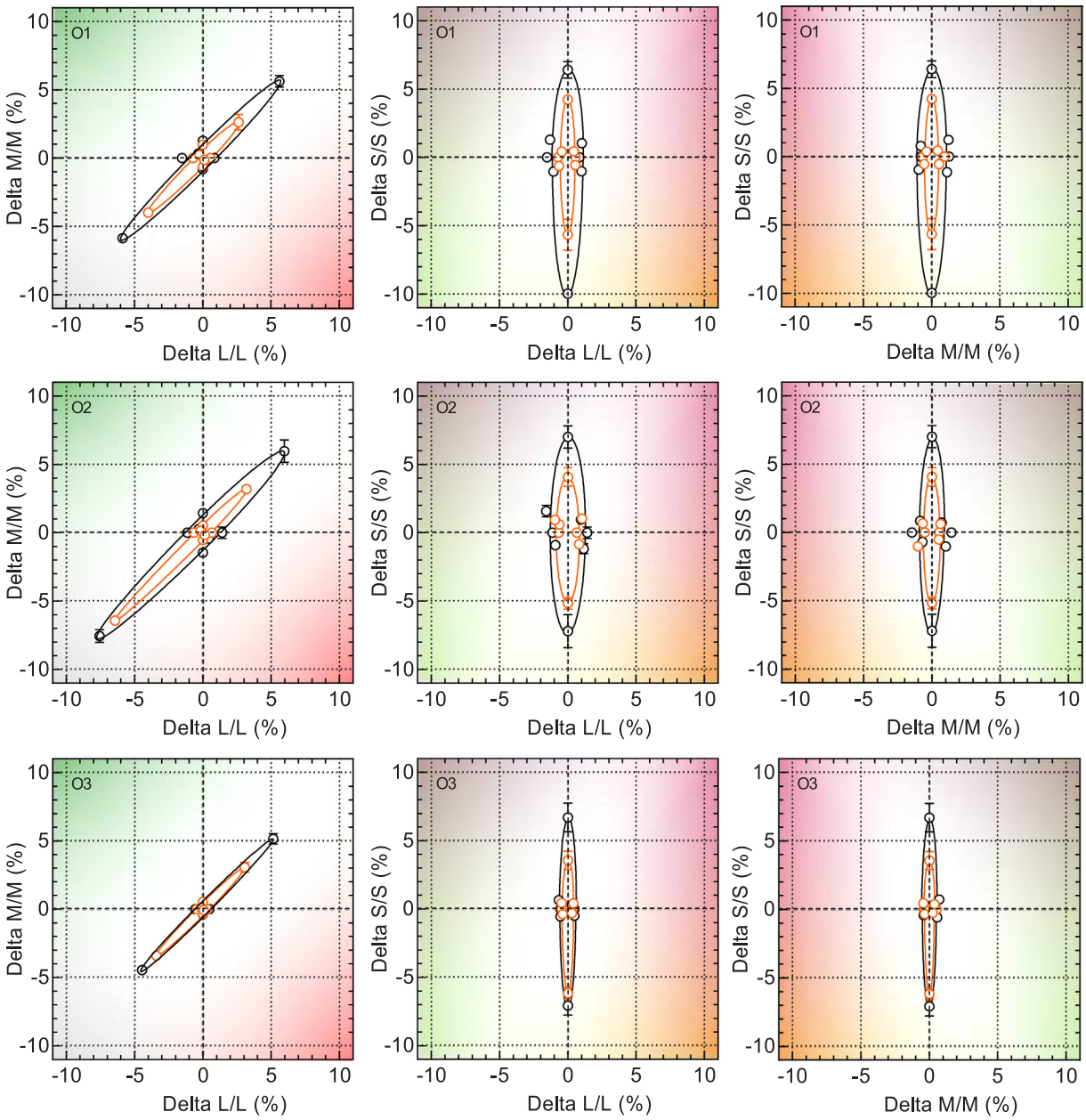

Fig. 2. Cone-mediated chromatic discrimination in peripheral retina. Threshold measurements and ellipses (solid line) defined by a quadratic model for three observers (O1, O2, O3) measured with constant melanopsin excitation (black symbols) and in the presence of an increment in melanopsin excitation (17% Weber contrast; orange symbols). The colour planes are specified in cone Trolands to allow direct comparison between the quantal excitations of the L-, M- and S-cone photoreceptors in terms of detection and discrimination. In the control condition (no change in melanopsin excitation) the ellipse orientations and thresholds show good agreement with those reported in the colour science literature. Error bars (SEM) are displayed when larger than the symbol. Data were measured in a 3-AFC paradigm with temporal white noise (40% Michelson contrast modulating L- M- and S-cones and Rod with no change in melanopsin excitation). (For interpretation of the references to colour in this figure legend, the reader is referred to the web version of this article.)

vision could be explained by an artefact originating from the melanopsin-directed stimulus; given that low contrast stimuli at or below visual threshold can lead to subthreshold summation (Foley, 1994; Graham, 1989), we examined the prospect that intrusion from non-melanopsin photoreceptor absorptions could explain the enhancement of the cone contrast discrimination threshold. To evaluate the magnitude of any such intrusions, we quantified the effect of the penumbral cone contrast resulting from attenuation of the melanopsin-directed stimulus by the retinal vasculature, and the variability in the open-field cone photoreceptor isolation produced by differences between the theoretical and physical light output of the photostimulator. A penumbral cone contrast pedestal and an open-field cone contrast pedestal were generated and chromatic discrimination remeasured along the three major cone axes (n = 3 observers); for all three axes, the difference between the detection threshold and that measured with each of the two pedestal types was negligible (Fig. 3C), and so the contrast enhancement cannot be explained by artefacts produced by the minor inaccuracies in our photoreceptor isolations. The L-, M- and S-cone and rod-directed temporal white noise is therefore sufficient to limit any such intrusions, if they were to exist. Importantly, the similarity of the detection thresholds between the trichromats and the deuteranomalous trichromatic observer (Fig. 3A; symbols with dots) indicates the individual observer calibration procedure can control for genetic polymorphisms affecting the cone photoreceptor spectral sensitivity; the application of a 10° CIE standard observer calibration with the deuteranomalous trichromatic observer (Fig. 3A; symbols with

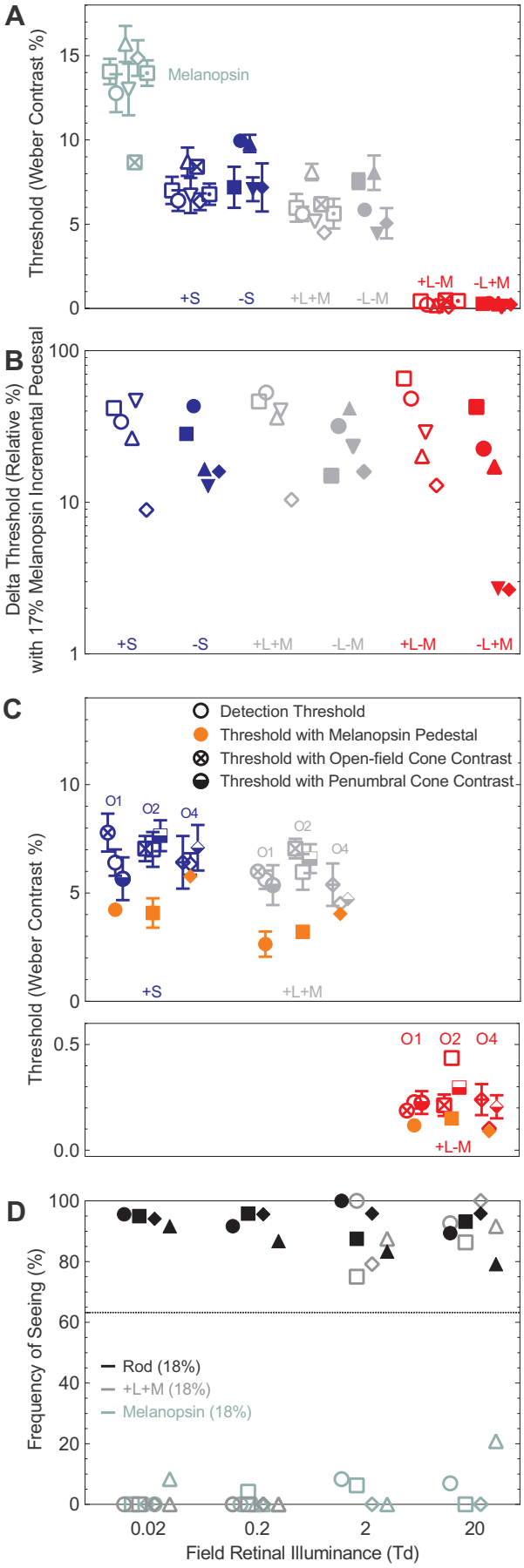

Fig. 3. Melanopsin enhancement of cone vision. (A) Detection threshold measurements for a melanopsin-directed increment (with no change in the rod and cone excitations) with temporal white noise to limit penumbral cone intrusions; cone-directed increment (open symbols) and decrement (closed symbols) thresholds are shown for each of the three primary cone axes. Data are for n = 6 observers (μ ± SEM), including five observers with trichromatic colour vision and one observer with deuteranomaly; the data for deuteranomalous observer denoted by symbols with the dot in the middle when using the individual observer calibration, and with a cross when using the CIE 10° standard observer calibration. (B) Relative percentage change in cone-directed stimulus thresholds in the presence of a 17% Weber contrast increment in melanopsin excitation (n = 5 observers with trichromatic colour vision). (C) Effects of non-melanopsin photoreceptor absorptions (i.e. failures in cone isolation or penumbral cone intrusion) on the enhancement (n = 3 observers). Error bars (SEM) are displayed when larger than the symbol. (D) Frequency of seeing (n = 4 observers) of 1000 ms duration (18% contrast) melanopsin-directed, rod-directed or +L + M cone-directed incremental pulses at scotopic and mesopic illumination levels; the 63.2% threshold probability of seeing is indicated by the horizontal dotted line.

crosses) results in a lower melanopsin threshold, indicative of cone intrusion, along with expected higher thresholds in the achromatic and chromatic directions (Dain & King-Smith, 1981). Fig. 3D shows that the rod-directed stimuli were suprathreshold at all four light levels (0.02–20 Td). The cone-directed stimuli were above threshold (63.2% frequency of seeing) at 2 and 20 Td whereas the melanopsin-directed stimuli were invisible at all four measured scotopic or mesopic illuminations; these findings indicate that any potential artefacts in the melanopsin- or cone-directed stimuli were not of sufficient contrast to be detected by the more sensitive rod pathway, and that melanopsin contributions to vision begin at a light level beyond 20 Td, and are evident at 200 Td (Zele, Feigl et al., 2018).

To determine if the enhancement of cone-mediated peripheral chromatic discrimination (Fig. 2) is a generalised effect independent of the melanopsin contrast, or part of the (so called) dipper component on a threshold versus contrast function, we measured cone-directed visual thresholds in the presence of spatially and temporally superimposed melanopsin pedestals of different contrasts (Fig. 4). The onset of the faciliatory effect occurred at ~9% melanopsin contrast (Fig. 4A), a level below melanopsin-directed contrast threshold (Fig. 3A), and was present until the highest measured contrast (22% melanopsin contrast); this faciliatory enhancement was manifest for all three canonical visual directions (Fig. 4B). The melanopsin-cone interaction returned a different contrast response pattern to that observed with typical, iso-luminant (+L + M stimulus and +L + M pedestal) and chromo-luminance conditions (+L + M stimulus and +S pedestal); the iso-luminant condition showed the expected dipper component at low pedestal contrasts followed by threshold masking at high contrasts; the crossed, chromo-luminance condition showed only a masking effect (Fig. 4C), as expected (Chen, Foley, & Brainard, 2000).

For both the +L + M and +S-cone pedestals conditions (Fig. 4C), the threshold versus contrast function returned a different response pattern to that observed for the cone-melanopsin interaction (Fig. 4A). A ~5% L + M pedestal contrast is required to produce an equivalent ~2.1% change in L + M threshold; > 11% melanopsin pedestal contrast is required to produce an equivalent L + M threshold change to that observed with the L + M pedestal (Fig. 4A). That the measured open field and penumbral L + M cone contrasts in the melanopsin pedestal are 0.1% and 0.7%, respectively (for a higher-contrast, 17% melanopsin pedestal), the facilitation cannot be explained by a luminance artefact (i.e. L + M signals in the melanopsin pedestal). In addition, the penumbral cone response is desensitised by the temporal white noise. Together, the L + M cone artefacts are insufficient to produce the facilitation effect. Similarly, the data in Fig. 3C show that cone-directed thresholds (+L + M, S, +L − M) measured in the presence of a pedestal having these open-field or penumbral cone contrasts

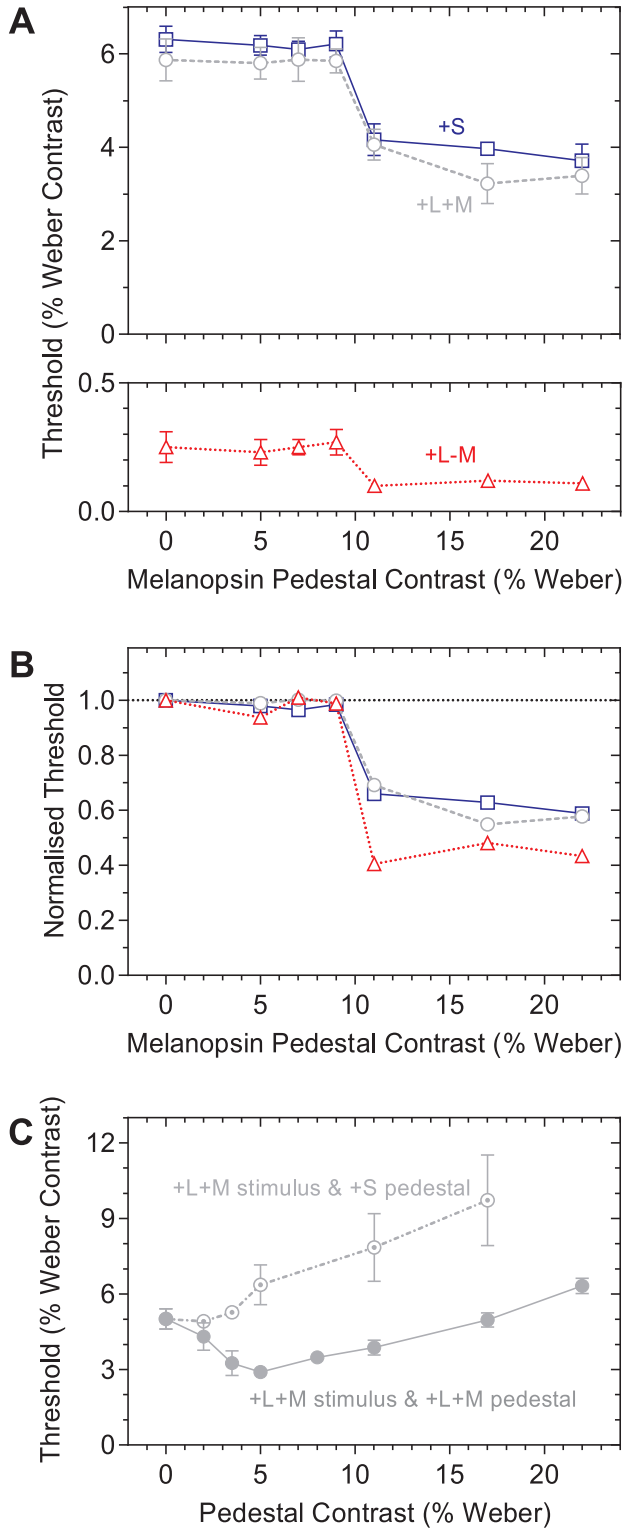

Fig. 4. Contrast response of the melanopsin interaction with cone vision. (A) Detection thresholds for each of the three primary cone axes (+L + M, S-cone and +L − M) measured in the presence of a variable contrast, melanopsin-directed incremental pedestal (5% − 22% contrast). There was no pedestal at zero pedestal contrast (i.e. baseline threshold). (B) Threshold versus contrast data normalised to baseline threshold. (C) Cone-only (control) conditions included an iso-luminant +L + M directed stimulus with a +L + M pedestal, and a chromo-luminance +L + M directed stimulus with a +S-cone pedestal. Symbols represent the average data of n = 3 observers (± SEM).

are not equivalent to the facilitation effect measured with a melanopsin pedestal.

4. Discussion

Here we show that human melanopsin photoreception with lower sensitivity than the canonical cone pathways (Fig. 3A) can confer a role for melanopsin in enhancing cone-mediated contrast discrimination in the peripheral retina (Figs. 2, 3B, 4B). This low melanopsin sensitivity is consistent with the diffuse expression of melanopsin photopigment along ipRGC dendrites and soma (Do et al., 2009). That melanopsin has a role in conscious vision is evident from human psychophysical investigations (Cao, Chang, & Gai, 2018; Spitschan et al., 2017; Zele, Adhikari et al., 2018; Zele, Feigl et al., 2018) and mouse models; the visual contrast sensitivity of melanopsin knockout mice is lower than in wild-type mice, with no change in their acuity (Schmidt et al., 2014), signifying the importance of melanopsin photoreception for supporting normal rod- and cone-mediated, mouse vision (Sonoda & Schmidt, 2016). In anticipating a role for melanopsin photoreception in human vision, melanopsin can provide rudimentary spatial vision in rod-cone knockout mice (Ecker et al., 2010). Melanopsin signals modulate mice dLGN neurons by increasing baseline firing rates (Davis, Eleftheriou, Allen, Procyk, & Lucas, 2015; Storchi et al., 2015), produce sustained, long-term firing for irradiance coding over extended durations (Brown et al., 2012) and increase the amplitude and response reproducibility of dLGN signals to fast visual responses (Storchi et al., 2015) that improves spatial frequency and temporal tuning (Allen et al., 2014). The contrast sensitivity (C_{50}) of mouse M4 ipRGCs to low spatial frequency (0.04–0.089 cycles per degree) drifting gratings (2 Hz) ranges from ~15% contrast in scotopic lighting to ~7% in photopic lighting, with lower C_{50} values in the wild-type than the melanopsin-knockout (Sonoda, Lee, Birnbaumer, & Schmidt, 2018), consistent with the lower cone contrast discrimination thresholds in the presence of the melanopsin pedestal. Even with slower temporal kinetics than cone photoreceptors, as evidenced from recordings in mice (Do et al., 2009) and non-human primate retina (Dacey et al., 2005), an ipRGC photoresponse is present in whole-mount (mouse) retina within 200 ms after onset of a 50 ms pulse (16.0 log quanta.cm^{-2}.s^{-1}). The ipRGC pathway can therefore process the short duration stimuli used in many psychophysical investigations, including the 1000 ms pulses used here. Psychophysical measurements also reveal lower temporal contrast sensitivity and critical flicker frequency for melanopsin photoreception than for cone-processing (Zele, Feigl et al., 2018), whereas short duration stimulus increments in the range of 4–16 ms produce reliable, non-image forming melanopsin-driven pupil responses (Joyce, Feigl, Cao, & Zele, 2015; Park et al., 2011).

For image-forming vision, an increase in melanopsin excitation that is time-locked to the cone-directed stimulus causes an interaction that produces a relative (%) change in L + M cone luminance, S-cone-mediated and +L − M cone mediated contrast sensitivity that increases on average by 36.6% (Fig. 3B). The data are not likely to be explained by inadvertent cone-contrast or rod-contrast in the melanopsin-directed stimulus (Fig. 3C, D); in any case, such an artefact would be expected to operate through a Weber's law like mechanism that produces a smaller, asymmetric effect in the opposite direction to that seen. The temporal white noise desensitises cone pathway sensitivity, but not melanopsin (Zele, Feigl et al., 2018), and so it could be posited that the melanopsin-directed pedestal undoes this desensitisation and restores sensitivity of the cone pathways; a mechanism through which melanopsin could restore cone vision has not however, been demonstrated. What then might be the reason(s) this melanopsin enhancement of cone-mediated vision has not been previously observed? Clearly, there was no direct evaluation of such effects, and so an assessment could be made only through post-hoc comparison of studies with similar outcome measures (e.g. detection or discrimination thresholds measured with spatio-temporal stimuli at the same, extra-foveal retinal eccentricity to

account for the absence of ipRGCs in the fovea), but potentially with light adaptation conditions producing different degrees of melanopsin excitation (a factor not historically specified in vision studies); the magnitude of such effects might however be expected to be small (i.e. not designed to generate large differences in melanopsin excitation) because vision experiments often use similar (usually three primary) stimulus generators and common adapting chromaticities (e.g. white appearing) to optimise the instrument gamut and dynamic range. The peak spectral response (~482 nm) of melanopsin in humans is between the rods and S-cones (Feigl & Zele, 2014) and so a three primary display will also cause the melanopsin excitation to vary with the cone and rod receptor-excitations, and the relative sensitivity of all photoreceptors classes will differ with the adapting chromaticity, a factor that was controlled in this study. Any such between-study comparisons also need to separate the effects of (real) individual differences from those arsing due to experimental error (Baraas & Zele, 2016; Mollon, Bosten, Peterzell, & Webster, 2017). Everything considered, cross-study data comparisons may not be suitable for effectively and precisely assessing the interactions between melanopsin and cone-mediated vision. Here, a repeated-measured design increased the study power and minimised the effects of individual differences on the outcome measure; this framework can be used to explore how melanopsin photoreception modulates cone and rod mediated vision under a broader set of experimental conditions.

The identification and naming of the hue, saturation and brightness of a colour (Berlin & Kay, 1969; Boynton & Olson, 1987) can be strongly affected by viewing context, including from different lights presented successively in view (Shevell & Kingdom, 2008). Between-observer differences in colour naming can be large and systematic for hue percepts assessed with hue scaling and when represented in cone-opponent and perceptual-opponent colour spaces (Emery, Volbrecht, Peterzell, & Webster, 2017). Individual selections of unique hues also vary between observers (Kuehni, 2004), especially with unique green (Volbrecht, Nerger, & Harlow, 1997). Given that many factors influence the connection between colour perception and colour naming, we developed a colour matching task to quantify the melanopsin-percept in terms of the cone photoreceptor excitations; the melanopsin-directed visual percept was found to have the equivalent consequence of the S-off L + M-on response property of ipRGCs (Zele, Feigl et al., 2018). Here, participants verbally described the melanopsin-directed stimulus as having an orangish or bluish-cyanish appearance. A range of hue labels for melanopsin-directed stimuli have been reported, including yellow-orange and greenish (Spitschan et al., 2017). When verbal reports were restricted to the four basic hues, an increase in melanopsin excitation was described as more greenish and yellowish, with variability between observers (Cao et al., 2018). These individual differences in the verbal reports might reflect variation in the degree of cone-intrusion in the stimulus and so we desensitised the cone (and rod) pathways through application of temporal white noise and included multiple control conditions to evaluate the prospect of non-melanopsin contributions to detection. Our working assumption was that these hue percepts result from the activation of a single photopigment, namely melanopsin. Although wavelength discrimination requires the spectral comparison of the outputs of at least two photoreceptors (Pokorny & Smith, 1970; Wright & Pitt, 1934), the precedence for anticipating non-cone-generated colour appearances mediated by a single photoreceptor class is established by the presence of variegated hue perception under dim, scotopic illumination, when only the rod photoreceptor is active (Elliott & Cao, 2013; Pokorny, Lutze, Cao, & Zele, 2006). Such rod-mediated hues include blues, bluish-greens, reds and oranges (Elliott & Cao, 2013; Nagel, 1924; Pokorny et al., 2006; Shin, Yaguchi, & Shioiri, 2004), with the object colour appearance changing depending on the scotopic luminance of other samples in the scene (Pokorny et al., 2006); the probable colour of these rod-mediated, relational hue percepts, may be inferred based on a person's prior natural visual experience (Pokorny et al., 2006) and involve top-down, cortical processes (Elliott & Cao, 2013). If melanopsin-directed stimuli give rise to hue perception, then it may involve cortical processes.

It is thought that melanopsin can input to all three primary retinogeniculate pathways as demonstrated in principal component analyses of natural images (Barrionuevo & Cao, 2014) and hue scaling experiments showing melanopsin activation alters the equilibrium point of the colour opponent (+L-M, S-cone) pathways to affect unique white settings (Cao et al., 2018). Moreover, the solar day produces cyclic changes in the environmental radiance and spectral light distribution and ipRGCs provide the primary photic input to entrain circadian rhythms (Berson, Dunn, & Takao, 2002), with the detectability of light varying throughout the day (Bassi & Powers, 1986), as does the human pupil light response (Zele et al., 2011), and so the importance of melanopsin activation in these processes needs to be further assessed. We quantified the cone-melanopsin interaction in the chromatic discrimination experiment at a single contrast level under stimulus conditions near the operational limit of our instrument stimulus gamut (Fig. 2). By further evaluating the contrast dependence of this interaction with a threshold versus contrast analysis (Fig. 4), we observed the facilitation of stimuli mediated via the canonical visual pathways is a more generalised facilitation effect that onsets at ~9% melanopsin contrast and is sustained until the maximum measured melanopsin contrast. The transition between two states might signify the activity of a non-linear process, sometimes called a hard threshold (Kontsevich & Tyler, 1999; Stockman & Plummer, 1998) that's beneficial in supressing noise (Kontsevich & Tyler, 1999). Background noise in the signal could be limited by the high isomerisation quantum yield and low thermal isomerisation rate of the melanopsin photopigment (Rinaldi, Melaccio, Gozem, Fanelli, & Olivucci, 2014). Between 10 and 22% melanopsin pedestal contrast, the normalised cone-mediated thresholds have an average slope of ~0.5 (Fig. 4B), but it remains to be seen if such behaviour continues at higher contrasts (outside our instrument gamut), or if the slope increases as observed in threshold versus contrast data with cone-directed pedestals (Fig. 4C). Flicker pupil responses with melanopsin and cone-directed stimuli also show adaptation responses that are weaker than typical Weber adaptation (Barrionuevo & Cao, 2016). We infer this improvement in photopic vision might be controlled by a process whereby melanopsin modulates the gain of the post-receptoral cone pathways, perhaps through a change in the positive slope of the accelerating contrast response function that defines contrast discrimination (Foley, 1994); consistent with this idea, ipRGCs can modulate the gain of retinal ganglion cells in mice retina to adjust information flow through the optic nerve to the brain (Milosavljevic et al., 2018).

Our evidence for an interaction between melanopsin and the L-, M- and S-cone photoreceptors indicates it may exist at a retinal site. In mouse retina, ipRGCs provide feedback to outer retinal photoreceptors via dopaminergic amacrine cells to modulate light adaptation (Zhang et al., 2008) and signal to several types of non-dopaminergic amacrine cells, via gap junctions (Reifler et al., 2015), in addition to feedforward signals via bipolar cells (Newkirk, Hoon, Wong, & Detwiler, 2013). Melanopsin phototransduction enhances the contrast sensitivity of the M4 ipRGC subtype that has a purported role in image formation in mice (Sonoda et al., 2018), together supporting the assertion that the source of the cone/melanopsin interaction is within the retina. In non-human primate retina, the pathway may include DB6 diffuse bipolar cells that transmit L- and M-cone signals to ipRGCs (Grünert, Jusuf, Lee, & Nguyen, 2011), with some connections to S-cones (Dacey, Crook, & Packer, 2014; Lee, Jusuf, & Grünert, 2004). ipRGC modulation of rod-cone circuits has also been demonstrated within the human retina (Hankins & Lucas, 2002). Although an fMRI study detected a change in the activity of human V1 to melanopsin-directed light stimulation (Spitschan et al., 2017), there is currently no anatomical or physiological data upon which to speculate a thalamic or higher visual locus for these melanopsin and cone interactions. It is important to highlight however, that our evidence for melanopsin photoreception and its

interaction with cone signals is not inconsistent with the trichromatic generalisation nor the standard observer colour matching functions which are dependent on the spectral absorbance of the L-, M- and S-cone spectral sensitivities (Smith & Pokorny, 1975). Instead, the anatomical and physiological data point towards a post-receptoral interaction site for these interactions (i.e. a second or higher order stage/zone; (Judd, 1949)).

Declaration of Competing Interest

The authors declare no competing financial interests.

Acknowledgements

Supported by the Australian Research Council Discovery Projects ARC-DP170100274 (AJZ, BF and DC) and Australian Research Council Future Fellowship ARC-FT180100458 (AJZ).

References

Adhikari, P., Feigl, B., & Zele, A. J. (2016). Rhodopsin and melanopsin contributions to the early redilation phase of the post-illumination pupil response (PIPR). *PLoS One, 11*(8), e0161175. https://doi.org/10.1371/journal.pone.0161175.

Adhikari, P., Zele, A. J., & Feigl, B. (2015). The Post-Illumination Pupil Response (PIPR). *Investigative Ophthalmology and Visual Science, 56*(6), 3838–3849.

Allen, A. E., Storchi, R., Martial, F. P., Bedford, R. A., & Lucas, R. J. (2017). Melanopsin contributions to the representation of images in the early visual system. *Current Biology, 27*(11) 1623 1632.e4.

Allen, A. E., Storchi, R., Martial, F. P., Petersen, R. S., Montemurro, M. A., Brown, T. M., & Lucas, R. J. (2014). Melanopsin-driven light adaptation in mouse vision. *Current Biology, 24*(21), 2481–2490.

Baraas, R. C., & Zele, A. J. (2016). Psychophysical correlates of retinal processing. In J. Kremers, R. C. Baraas, & N. J. Marshall (Eds.). *Human Color Vision* (pp. 133–157). Switzerland: Springer.

Barrionuevo, P. A., & Cao, D. (2014). Contributions of rhodopsin, cone opsins, and melanopsin to postreceptoral pathways inferred from natural image statistics. *Journal of the Optical Society of America A, 31*(4), A131–139.

Barrionuevo, P. A., & Cao, D. (2016). Luminance and chromatic signals interact differently with melanopsin activation to control the pupil light response. *Journal of Vision, 16*(11), 29.

Barrionuevo, P. A., Nicandro, N., McAnany, J. J., Zele, A. J., Gamlin, P., & Cao, D. (2014). Assessing rod, cone, and melanopsin contributions to human pupil flicker responses. *Investigative Ophthalmology and Visual Science, 55*(2), 719–727.

Bassi, C. J., & Powers, M. K. (1986). Daily fluctuations in the detectability of dim lights by humans. *Physiology and Behavior, 38*(6), 871–877.

Berlin, B., & Kay, P. (1969). *Basic Color Terms: Their Universality and Evolution.* Berkeley: University of California Press.

Berson, D. M., Dunn, F. A., & Takao, M. (2002). Phototransduction by retinal ganglion cells that set the circadian clock. *Science, 295*(5557), 1070–1073.

Boynton, R. M., & Kambe, N. (1980). Chromatic difference steps of moderate size measured along theoretically critical axes. *Color Research and Application, 5*, 13–23.

Boynton, R. M., & Olson, C. X. (1987). Locating basic colors in the OSA space. *Color Research and Application, 12*, 94–105.

Brindley, G. S., Du Croz, J. J., & Rushton, W. A. (1966). The flicker fusion frequency of the blue-sensitive mechanism of colour vision. *Journal of Physiology, 183*(2), 497–500.

Brown, T. M., Tsujimura, S., Allen, A. E., Wynne, J., Bedford, R., Vickery, G., ... Lucas, R. J. (2012). Melanopsin-based brightness discrimination in mice and humans. *Current Biology, 22*(12), 1134–1141.

Burns, S. A., & Elsner, A. E. (1993). Color matching at high illuminances: Photopigment optical density and pupil entry. *Journal of the Optical Society of America A, 10*, 221–230.

Burns, S. A., Elsner, A. E., Lobes, L. A., Jr., & Doft, B. H. (1987). A psychophysical technique for measuring cone photopigment bleaching. *Investigative Ophthalmology and Visual Science, 28*, 711–717.

Cao, D., Chang, A., & Gai, S. (2018). Evidence for an impact of melanopsin activation on unique white perception. *Journal of the Optical Society of America A, 35*(4), B287–B291.

Cao, D., Nicandro, N., & Barrionuevo, P. A. (2015). A five-primary photostimulator suitable for studying intrinsically photosensitive retinal ganglion cell functions in humans. *Journal of Vision, 15*(1) 15 11 27.

Cao, D., Pokorny, J., Smith, V. C., & Zele, A. J. (2008). Rod contributions to color perception: Linear with rod contrast. *Vision Research, 48*(26), 2586–2592.

Chen, C., Foley, J. M., & Brainard, D. H. (2000). Detection of chromoluminance patterns on chromoluminance pedestals I: Threshold measurements. *Vision Research, 40*, 773–788.

CIE (1994). Light as a true visual quantity: Principles of measurement. Publ. CIE No.41. Bureau Central de la CIE, Paris (pp. TC-1.4).

Cole, G. R., Hine, T., & McIlhagga, W. (1993). Detection mechanisms in L-, M-, and S-cone contrast space. *Journal of the Optical Society of America A, 10*(1), 38–51.

Dacey, D. M., Crook, J. D., & Packer, O. S. (2014). Distinct synaptic mechanisms create parallel S-ON and S-OFF color opponent pathways in the primate retina. *Visual Neuroscience, 31*(2), 139–151.

Dacey, D. M., Liao, H. W., Peterson, B. B., Robinson, F. R., Smith, V. C., Pokorny, J., ... Gamlin, P. D. (2005). Melanopsin-expressing ganglion cells in primate retina signal colour and irradiance and project to the LGN. *Nature, 433*(7027), 749–754.

Dain, S. J., & King-Smith, P. E. (1981). Visual thresholds in dichromats and normals; the importance of post-receptoral processes. *Vision Research, 21*(4), 573–580.

Davis, K. E., Eleftheriou, C. G., Allen, A. E., Procyk, C. A., & Lucas, R. J. (2015). Melanopsin-derived visual responses under light adapted conditions in the mouse dLGN. *PLoS One, 10*(3), e0123424.

Do, M. T., Kang, S. H., Xue, T., Zhong, H., Liao, H. W., Bergles, D. E., & Yau, K. W. (2009). Photon capture and signalling by melanopsin retinal ganglion cells. *Nature, 457*(7227), 281–287.

Ecker, J. L., Dumitrescu, O. N., Wong, K. Y., Alam, N. M., Chen, S. K., LeGates, T., ... Hattar, S. (2010). Melanopsin-expressing retinal ganglion-cell photoreceptors: Cellular diversity and role in pattern vision. *Neuron, 67*(1), 49–60.

Elliott, S. L., & Cao, D. (2013). Scotopic hue percepts in natural scenes. *Journal of Vision, 13*(13), 15–16. https://doi.org/10.1167/13.13.15.

Emery, K. J., Volbrecht, V. J., Peterzell, D. H., & Webster, M. A. (2017). Variations in normal color vision. VII. Relationships between color naming and hue scaling. *Vision Research, 141*, 66–75.

Enezi, J., Revell, V., Brown, T., Wynne, J., Schlangen, L., & Lucas, R. (2011). A "melanopic" spectral efficiency function predicts the sensitivity of melanopsin photoreceptors to polychromatic lights. *Journal of Biological Rhythms, 26*(4), 314–323.

Estévez, O., & Spekreijse, H. (1982). The "silent substitution" method in visual research. *Vision Research, 22*(6), 681–691.

Feigl, B., & Zele, A. J. (2014). Melanopsin-expressing intrinsically photosensitive retinal ganglion cells in retinal disease. *Optometry and Vision Science, 91*(8), 894–903.

Foley, J. M. (1994). Human luminance pattern-vision mechanisms: Masking experiments require a new model. *Journal of the Optical Society of America A, 11*, 1710–1719.

Gamlin, P. D., McDougal, D. H., Pokorny, J., Smith, V. C., Yau, K. W., & Dacey, D. M. (2007). Human and macaque pupil responses driven by melanopsin-containing retinal ganglion cells. *Vision Research, 47*(7), 946–954.

Gooley, J. J., Ho Mien, I., St Hilaire, M. A., Yeo, S. C., Chua, E. C., van Reen, E., ... Lockley, S. W. (2012). Melanopsin and rod-cone photoreceptors play different roles in mediating pupillary light responses during exposure to continuous light in humans. *Journal of Neuroscience, 32*(41), 14242–14253.

Graham, N. V. S. (1989). *Visual Pattern Analyzers.* New York: Oxford University Press.

Grünert, U., Jusuf, P. R., Lee, S. C., & Nguyen, D. T. (2011). Bipolar input to melanopsin containing ganglion cells in primate retina. *Visual Neuroscience, 28*(1), 39–50.

Guth, S. L., & Lodge, H. R. (1973). Heterochromatic additivity, foveal spectral sensitivity, and a new color model. *Journal of the Optical Society of America, 63*(4), 450–462.

Hankins, M. W., & Lucas, R. J. (2002). The primary visual pathway in humans is regulated according to long-term light exposure through the action of a nonclassical photopigment. *Current Biology, 12*(3), 191–198.

Hannibal, J., Kankipati, L., Strang, C. E., Peterson, B. B., Dacey, D., & Gamlin, P. D. (2014). Central projections of intrinsically photosensitive retinal ganglion cells in the macaque monkey. *Journal of Comparative Neurology, 522*(10), 2231–2248.

Hathibelagal, A. R., Feigl, B., Cao, D., & Zele, A. J. (2018). Extrinsic cone-mediated postreceptoral noise inhibits the rod temporal impulse response function. *Journal of the Optical Society of America A, 35*(4), B72–B77.

Hathibelagal, A. R., Feigl, B., Kremers, J., & Zele, A. J. (2016). Correlated and uncorrelated invisible temporal white noise alters mesopic rod signaling. *Journal of the Optical Society of America A, 33*(3), A93–103.

Horiguchi, H., Winawer, J., Dougherty, R. F., & Wandell, B. A. (2013). Human trichromacy revisited. *Proceeding of the National Academy of Sciences USA, 110*(3), E260–269.

Joyce, D. S., Feigl, B., Cao, D., & Zele, A. J. (2015). Temporal characteristics of melanopsin inputs to the human pupil light reflex. *Vision Research, 107*, 58–66.

Judd, D. B. (1934). Response functions for types of vision according to the Müller Theory. *Journal of Research of the National Bureau of Standards, 42*(1), 1–16.

Kontsevich, L. L., & Tyler, C. W. (1999). Nonlinearities of near-threshold contrast transduction. *Vision Research, 39*(10), 1869–1880.

Krauskopf, J., Williams, D. R., & Heeley, D. W. (1982). Cardinal directions of color space. *Vision Research, 22*(9), 1123–1131.

Kuehni, R. G. (2004). Variability in unique hue selection: A surprising phenomenon. *Color Research and Application, 29*(2), 158–162.

Lee, S. C., Jusuf, P. R., & Grünert, U. (2004). S-cone connections of the diffuse bipolar cell type DB6 in macaque monkey retina. *Journal of Comparative Neurology, 474*(3), 353–363.

Lee, B. B., Pokorny, J., Smith, V. C., Martin, P. R., & Valberg, A. (1990). Luminance and chromatic modulation sensitivity of macaque ganglion cells and human observers. *Journal of the Optical Society of America A, 7*(12), 2223–2236.

Milosavljevic, N., Storchi, R., Eleftheriou, C. G., Colins, A., Petersen, R. S., & Lucas, R. J. (2018). Photoreceptive retinal ganglion cells control the information rate of the optic nerve. *Proceeding of the National Academy of Sciences USA, 115*(50), E11817–E11826.

Mollon, J. D., Bosten, J. M., Peterzell, D. H., & Webster, M. A. (2017). Individual differences in visual science: What can be learned and what is good experimental practice? *Vision Research, 141*, 4–15.

Nagel, W. (1924). Appendix: Adaptation, Twilight Vision and the Duplicity Theory. In J. P. C. Southall (Ed.). *Helmholtz's Treatise on Physiological OpticsTranslated from the Third German* (pp. 313–343). Rochester, New York: Optical Society of America.

Newkirk, G. S., Hoon, M., Wong, R. O., & Detwiler, P. B. (2013). Inhibitory inputs tune the light response properties of dopaminergic amacrine cells in mouse retina. *Journal if Neurophysiology, 110*(2), 536–552.

Park, J. C., Moura, A. L., Raza, A. S., Rhee, D. W., Kardon, R. H., & Hood, D. C. (2011).

Toward a clinical protocol for assessing rod, cone, and melanopsin contributions to the human pupil response. *Investigative Ophthalmology and Visual Science, 52*(9), 6624–6635.
Pelli, D. G. (1985). Uncertainty explains many aspects of visual contrast detection and discrimination. *Journal of the Optical Society of America A, 2*(9), 1508–1532.
Pokorny, J., Jin, Q., & Smith, V. C. (1993). Spectral-luminosity functions, scalar linearity, and chromatic adaptation. *Journal of the Optical Society of America A, 10*(6), 1304–1313.
Pokorny, J., Lutze, M., Cao, D., & Zele, A. J. (2006). The color of night: Surface color perception under dim illuminations. *Visual Neuroscience, 23*(3–4), 525–530.
Pokorny, J., & Smith, V. C. (1970). Wavelength discrimination in the presence of added chromatic fields. *Journal of the Optical Society of America A, 60*(4), 562–569.
Reifler, A. N., Chervenak, A. P., Dolikian, M. E., Benenati, B. A., Li, B. Y., Wachter, R. D., ... Wong, K. Y. (2015). All spiking, sustained ON displaced amacrine cells receive gap-junction input from melanopsin ganglion cells. *Current Biology, 25*(21), 2878.
Rinaldi, S., Melaccio, F., Gozem, S., Fanelli, F., & Olivucci, M. (2014). Comparison of the isomerization mechanisms of human melanopsin and invertebrate and vertebrate rhodopsins. *Proceeding of the National Academy of Sciences USA, 111*(5), 1714–1719.
Schmidt, T. M., Alam, N. M., Chen, S., Kofuji, P., Li, W., Prusky, G. T., & Hattar, S. (2014). A role for melanopsin in alpha retinal ganglion cells and contrast detection. *Neuron, 82*(4), 781–788.
Shapiro, A. G., Pokorny, J., & Smith, V. C. (1996). Cone-rod receptor spaces with illustrations that use CRT phosphor and light-emitting-diode spectra. *Journal of the Optical Society of America A, 13*(12), 2319–2328.
Sharpe, L. T., Stockman, A., Jagla, W., & Jägle, H. (2010). A luminous efficiency function, VD*65 (lambda) for daylight adaptation: A correction. *Color Research and Application, 636*(1), 43–46.
Shevell, S. K., & Kingdom, F. A. (2008). Color in complex scenes. *Annual Review of Psychology, 59*, 143–166.
Shin, J. C., Yaguchi, H., & Shioiri, S. (2004). Change of color appearance in photopic, mesopic and scotopic vision. *Optical Review, 11*(4), 265–271.
Smith, V. C., & Pokorny, J. (1975). Spectral sensitivity of the foveal cone photopigments between 400 and 500 nm. *Vision Research, 15*(2), 161–171.
Sonoda, T., Lee, S. K., Birnbaumer, L., & Schmidt, T. M. (2018). Melanopsin phototransduction is repurposed by ipRGC subtypes to shape the function of distinct visual circuits. *Neuron, 99*(4), 754–767 e754.
Sonoda, T., & Schmidt, T. M. (2016). Re-evaluating the role of intrinsically photosensitive retinal ganglion cells: New roles in image-forming functions. *Integrative and Comparative Biology, 56*(5), 834–841.
Spitschan, M., Aguirre, G. K., & Brainard, D. H. (2015). Selective stimulation of penumbral cones reveals perception in the shadow of retinal blood vessels. *PLoS One, 10*(4), e0124328.
Spitschan, M., Bock, A. S., Ryan, J., Frazzetta, G., Brainard, D. H., & Aguirre, G. K. (2017). The human visual cortex response to melanopsin-directed stimulation is accompanied by a distinct perceptual experience. *Proceeding of the National Academy of Sciences USA, 114*(46), 12291–12296.
Spitschan, M., Jain, S., Brainard, D. H., & Aguirre, G. K. (2014). Opponent melanopsin and S-cone signals in the human pupillary light response. *Proceeding of the National Academy of Sciences USA, 111*(43), 15568–15572.
Stockman, A., & Plummer, D. J. (1998). Color from invisible flicker: A failure of the Talbot-Plateau law caused by an early 'hard' saturating nonlinearity used to partition the human short-wave cone pathway. *Vision Research, 38*, 3703–3728.
Storchi, R., Milosavljevic, N., Eleftheriou, C. G., Martial, F. P., Orlowska-Feuer, P., Bedford, R. A., ... Lucas, R. J. (2015). Melanopsin-driven increases in maintained activity enhance thalamic visual response reliability across a simulated dawn. *Proceeding of the National Academy of Sciences USA, 112*(42), E5734–5743.
Swanson, W. H., Ueno, T., Smith, V. C., & Pokorny, J. (1987). Temporal modulation sensitivity and pulse detection thresholds for chromatic and luminance perturbations. *Journal of the Optical Society of America A, 4*, 1992–2005.
Volbrecht, V. J., Nerger, J. L., & Harlow, C. E. (1997). The bimodality of unique green revisited. *Vision Research, 37*(4), 407–416.
Wright, W. D. (1936). Hue discrimination and its relation to the adaptation of the eye. *Journal of Physiology, 88*(2), 167–175.
Wright, W. D., & Pitt, F. H. G. (1934). Hue-discrimination in normal colour-vision. *Proceedings of the Physical Society (London), 46*(3), 459–473. https://doi.org/10.1088/0959-5309/46/3/317.
Zele, A. J., Adhikari, P., Cao, D., & Feigl, B. (2019). Melanopsin and cone photoreceptor inputs to the afferent pupil light response. *Frontiers in Neurology, 10*, 529. https://doi.org/10.3389/fneur.2019.00529.
Zele, A. J., Adhikari, P., Feigl, B., & Cao, D. (2018a). Cone and melanopsin contributions to human brightness estimation. *Journal of the Optical Society of America A, 35*(4), B19–B25.
Zele, A. J., Feigl, B., Adhikari, P., Maynard, M. L., & Cao, D. (2018b). Melanopsin photoreception contributes to human visual detection, temporal and colour processing. *Scientific Reports, 8*(1), 3842. https://doi.org/10.1038/s41598-018-22197-w.
Zele, A. J., Feigl, B., Kambhampati, P. K., Aher, A., McKeefry, D., Parry, N., ... Kremers, J. (2017). A temporal white noise analysis for extracting the impulse response function of the human electroretinogram. *Translational Vision Science and Technology, 6*(6), 1–15. https://doi.org/10.1167/tvst.6.6.1.
Zele, A. J., Feigl, B., Smith, S. S., & Markwell, E. L. (2011). The circadian response of intrinsically photosensitive retinal ganglion cells. *PLoS One, 6*(3), e17860. https://doi.org/10.1371/journal.pone.0017860.
Zele, A. J., Smith, V. C., & Pokorny, J. (2006). Spatial and temporal chromatic contrast: Effects on chromatic discrimination for stimuli varying in L- and M-cone excitation. *Visual Neuroscience, 23*(3–4), 495–501.
Zhang, D. Q., Wong, K. Y., Sollars, P. J., Berson, D. M., Pickard, G. E., & McMahon, D. G. (2008). Intraretinal signaling by ganglion cell photoreceptors to dopaminergic amacrine neurons. *Proceeding of the National Academy of Sciences USA, 105*(37), 14181–14186.